

Modulation of MRP-1-Mediated Multidrug Resistance by Indomethacin Analogues

Claudia Rosenbaum,[†] Sonja Röhrs,[‡] Oliver Müller,^{‡,§} and Herbert Waldmann^{*,†}

Abteilung Chemische Biologie and Abteilung Strukturelle Biologie, Max-Planck-Institut für Molekulare Physiologie, Otto-Hahn-Strasse 11, 44227 Dortmund, Germany, and Organische Chemie, Universität Dortmund, Fachbereich 3, 44227 Dortmund, Germany

Received February 2, 2004

Multidrug resistance (MDR) is a major limiting factor in the development and application of drug candidates. MDR caused by MRP-1 is known to be modulated by the nonsteroidal antiinflammatory drug indomethacin. We have synthesized and biologically evaluated a library of indomethacin analogues. The indomethacin-derived compound library was synthesized employing the Fischer–indole synthesis as the key transformation and making use of a “resin-capture-release” strategy. Sixty representative members of the library were evaluated in a cell biological cytotoxicity assay employing the MRP-1 expressing human glioblastoma cell line T98G as a model system. Nine of the 60 tested derivatives increased the doxorubicin-mediated cytotoxicity at a comparable or higher level than indomethacin itself. Analysis of these derivatives revealed an interesting structure–function relationship. Most remarkably, two substances increased the toxicity, when doxorubicin was used at clinically relevant low concentrations, at a higher degree than indomethacin.

Introduction

A large number of clinically observed resistance of cancers to chemically unrelated cytotoxic compounds is caused by the overexpression of multidrug transporter proteins in the tumor cell membrane. Multidrug resistance (MDR) describes the property of a cell to develop resistance against the effects of a certain external compound and in some cases also against structurally and functionally different compounds. Many heterocyclic natural compounds, which are used in tumor therapy, can cause MDR. Among these are the alkaloids daunorubicin, doxorubicin, and vincristine. MDR can result in a significant efficiency decrease of chemotherapy. Many studies have analyzed the development of MDR in different cell types. The best characterized mechanism of MDR is the overexpression of the gene MDR-1, which codes for the transmembrane protein phosphoglycoprotein P-170.¹ This protein works as an ATP-dependent pump and is able to lower the intracellular concentration of several cytotoxic compounds. P-170 shows a sequence similarity of 15–19% to the family of multidrug resistance associated proteins (MRPs), which consists of at least seven homologous members.² MRPs are able to cause MDR, which is independent from P-170.³ The 190 kDa MRP-1 is found in normal human and tumor tissues. On the basis of their sequence homologies P-170 and the MRP family belong to the class of transmembrane ABC transporters.⁴ P-170 and MRP-1 have similar mechanisms of drug export.⁵ The

major MDR proteins are highly promiscuous transporters; they share the ability of recognizing and translocating a large number of various, mainly hydrophobic compounds. In addition to their overlapping substrate specificity, each transporter can handle unique compounds. P-170 is a transporter for large hydrophobic either uncharged or slightly positively charged compounds, while the MRP family is mostly transporting hydrophobic anionic conjugates and also uncharged drugs. MRP mediates also the transport of partially detoxified compounds, such as glutathione and glucuronide conjugates.⁶ Compounds such as verapamil or cyclosporine can circumvent P-170-mediated MDR. However, clinical studies failed to meet expectations because the use of these drugs in a combined chemotherapy caused severe negative side effects.⁷ Until today there are few data about MDR caused by MRP-1 and its circumvention.⁸ Thus, the development of potent and nontoxic agents, which unfold minimal side effects, to inhibit MRP-1-induced MDR belongs to the crucial aims of medical and pharmacological research. Recently nonsteroidal antiinflammatory drugs (NSAIDs) turned into the focus of medical interest because of their high potential as agents in cancer prevention.⁹ Several studies analyzed the NSAID-induced increase of chemotherapeutic toxicity.¹⁰ These studies show that MRP-1 activity can be modulated by treatment with the NSAID indomethacin (**1**).¹¹ One possible explanation for this modulation is a direct interaction between indomethacin and MRP-1 and the competitive inhibition of MRP-1. This model is supported by the fact that indomethacin with a $pK_a = 4.1$ is negatively charged at physiological pH and that MRP-1 shows a preference for hydrophilic compounds and transports amphiphilic organic anions.^{12,5} Studies with indomethacin have also shown that MDR is probably not caused by the inhibition of glutathione-S-transferase (GST). Compounds, which are

* To whom correspondence should be addressed. Phone: +49-231-133-2400. Fax: +49-231-133-2499. E-mail: herbert.waldmann@mpi-dortmund.mpg.de.

[†] Abteilung Chemische Biologie, Max-Planck-Institut für Molekulare Physiologie, and Universität Dortmund.

[‡] Abteilung Strukturelle Biologie, Max-Planck-Institut für Molekulare Physiologie.

[§] Phone: +49-231-133-2158. Fax: +49-231-133-2199. E-mail: oliver.mueller@mpi-dortmund.mpg.de.

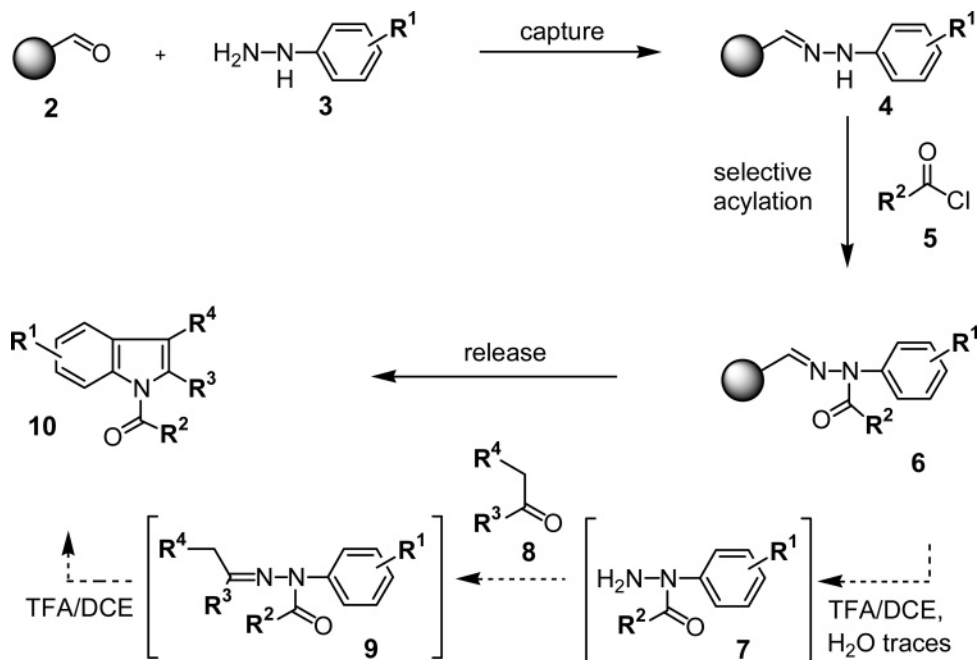
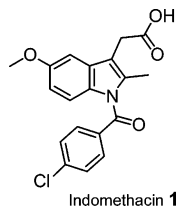


Figure 1. Three-step synthesis of the indomethacin library by a resin "capture-and-release" methodology.

unable to inhibit GST, can still inhibit cellular detoxification to a level similar to that of indomethacin.¹⁰ Correlations between MDR inhibition and the well-known inhibitory effects on the cyclooxygenase (COX) pathway by indomethacin could be excluded.^{13,14} Thus, the two isoforms of the COX enzyme COX-1 and COX-2 seem to play no relevant role in the mechanism of MDR inhibition. On the basis of the current data, indomethacin might serve as a promising amplifier of chemotherapeutic toxicity and might be suited for the combined cytostatic therapy of cancer types, which have developed MDR as a result of MRP-1 overexpression. In this study we analyzed the MDR modulation induced by novel indomethacin analogues in order to identify compounds which show stronger effects on MDR compared to indomethacin. To this end, we synthesized a library of indomethacin analogues in a solid-phase synthesis approach and characterized the compounds in a combined toxicity assay.



Results and Discussion

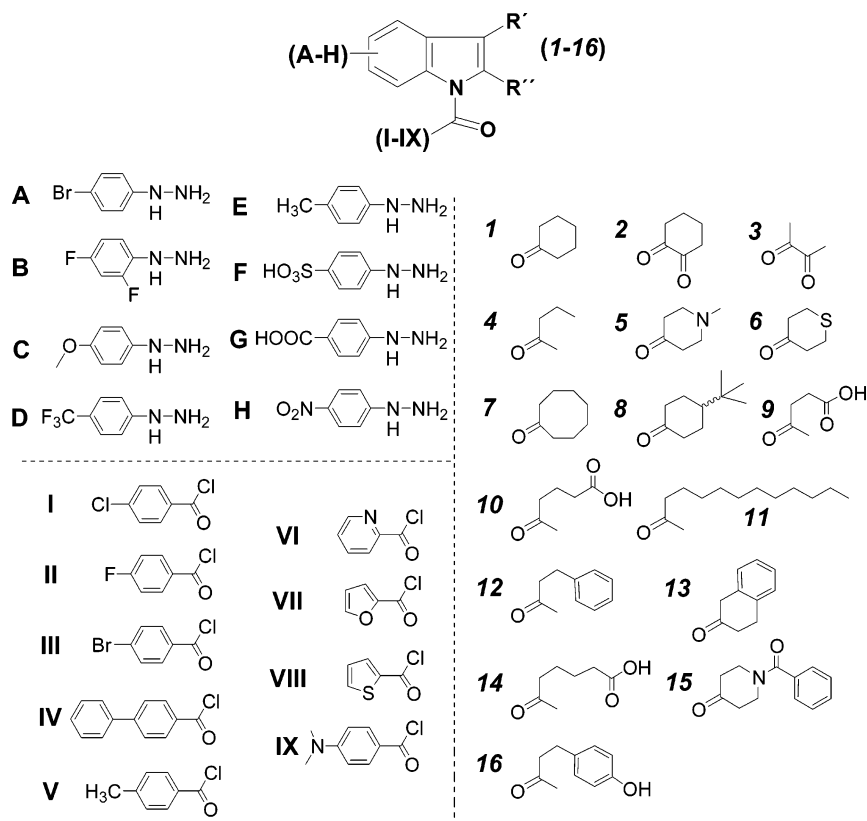
Chemistry. The indomethacin-derived compound library was synthesized by employing the Fischer–indole synthesis as a key step.¹⁵ To establish a particularly practical and efficient synthesis sequence, we resorted to a "resin-capture-release" strategy¹⁶ that made use of three types of readily available building blocks and circumvented permanent attachment to and final release from the solid support in additional synthesis steps.¹⁷

As shown in Figure 1 polystyrene aldehyde resin **2** (loading, 0.9 mmol·g⁻¹; obtained from Advanced

Chemtech) was condensed with hydrazines **3** to yield polymer-bound hydrazones **4**. In intermediates **4** the polymer serves as reagent-capturing auxiliary, allowing for easy removal of surplus reagent and as temporary blocking function for the terminal NH₂ group of the hydrazine. Regioselectively *N*-acylated hydrazones **6** obtained thereby are then subjected to treatment with acid and ketones **8** in the presence of water traces to yield the desired indole derivatives **10**. In this reaction sequence the water hydrolyzes the hydrazones and thereby releases selectively acylated hydrazines **7** into solution where they condense with ketones **8** to give hydrazone intermediates **9**. These then undergo a [3,3]-sigmatropic rearrangement under the reaction conditions, thereby shifting the equilibrium between the hydrazones **6** and **9** irreversibly to the desired side. This strategy employs ketones, acid chlorides, and hydrazines as building blocks which are either commercially available in a great variety or readily prepared by numerous well-established synthesis methods allowing for ready construction of a fairly diverse compound collection.

Figure 2 shows the building blocks used for the synthesis of a library of 197 indomethacin analogues (see the Supporting Information) in overall yields ranging from 4% to quantitative (see Table 1).

The results demonstrate that electron-withdrawing and -donating substituents can be incorporated in the hydrazine and the acid chloride. Electron-poor and -rich heterocycles are tolerated as well. Also the ketones may incorporate different heteroatom substituents. The use of hydrazine building blocks (**A–H**) and substituted benzoyl chlorides (**I–IX**) lead to formation of aromatic indoles, which carry the substituents in positions 5 and 7 and a *N*-benzoyl unit with different para-substituents reaching from sterically demanding and nonpolar biphenyl rings **IV** to *tert*-amines **IX**. The diversity of the used ketones (**1–16**) ranges from the hydrophilic laevulinic acid **9** as part of indomethacin to the very hydrophobic 2-tridecanone **11**. Not unexpectedly the overall yield was highest if activating electron-donating

**Figure 2.** Scheme of the library building blocks.**Table 1.** Results of the Library Synthesis

	yield ^a (%)		yield ^a (%)
A-I	45–100	C-IX	20–47
A-V	9–26	D-I	47
A-VII	62–100	E-I	40–90
B-I	21–60	F-I	4–58
C-I	19–45	F-IV	4–52
C-II	16–63	F-VI	15–20
C-III	32–81	F-VII	7–55
C-IV	15–81	F-VII I	11–66
C-VI	17–49	F-IX	10–29
C-VII	9–99	G-I	4–26
C-VII I	21–46	H-I	11–29

^a Yield ranges are given for the conversion of the respective *N*-acylated hydrazones with ketones (1–16). All yields refer to purified products (purity > 99% (HPLC, 215 nm)). The identities of the compounds were proven by means of LC-MS, GC-MS, NMR, and high-resolution mass spectra.

substituents were incorporated into the hydrazines, indicating the importance of two hydrazone formation reactions in the overall process. The use of the electronically activated phenylhydrazine blocks **C** and **E** resulted in very high yields. However, even in the presence of deactivating SO₃H, COOH, and NO₂ groups, the synthesis of *N*-acylated indoles via the “resin-capture-release” strategy was successful.

Depending on the ketone employed, the crude reaction products are obtained with purities of approximately 70 to >95%. After simple chromatography, all compounds were isolated in >99% purity.

These synthesis strategies gave rise to a complex and diverse indole library synthesized efficiently within a very short period of time. For the cell-based assay we first selected several representative compounds for each building block and combined them, in a positional

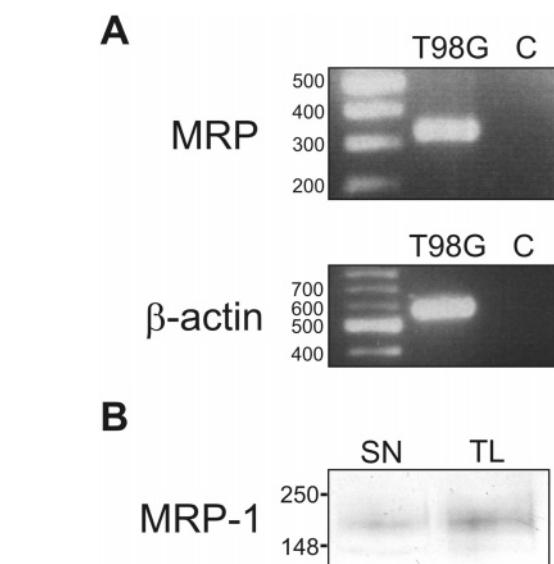


Figure 3. Analysis of MRP expression by RT-PCR and of the presence of the MRP-1 protein in T98G cells. (A) Upper, agarose gel of MRP transcript after reverse transcription and PCR amplification; lower, agarose gel of β-actin transcript after RT-PCR: M, 100 bp ladder marker; T98G, RNA from 98G cells; C, template-free negative control. The sizes of marker fragments are indicated in base pairs. (B) Western blot membrane probed with anti-MRP-1 antibody: SN, soluble supernatant; TL, total cell lysate of T98G cells. The sizes of molecular weight marker fragments are indicated in kilodaltons.

scanning mode, with the indomethacin core structure. We focused on the active substituents and selected compounds for the next cell assay based on these results. Over all 60 indomethacin analogues were evaluated in a combined toxicity assay (Table 2).

Table 2. List of Indomethacin Analogues Investigated in This Study

compd	R ¹	R ²	R ³ /R ⁴	name
1	C	I	9	[1-(4-chlorobenzoyl)-5-methoxy-2-methyl-1 <i>H</i> -indol-3-yl]acetic acid
2	C	II	9	[1-(4-fluorobenzoyl)-5-methoxy-2-methyl-1 <i>H</i> -indol-3-yl]acetic acid
3	C	III	9	[1-(4-bromobenzoyl)-5-methoxy-2-methyl-1 <i>H</i> -indol-3-yl]acetic acid
4	C	IV	9	[1-(biphenyl-4-carbonyl)-5-methoxy-2-methyl-1 <i>H</i> -indol-3-yl]acetic acid
5	C	V	9	[5-methoxy-2-methyl-1-(4-methylbenzoyl)-1 <i>H</i> -indol-3-yl]acetic acid
6	C	VI	9	[5-methoxy-2-methyl-1-(pyridine-2-carbonyl)-1 <i>H</i> -indol-3-yl]acetic acid
7	C	VII	3	1-[1-(furan-2-carbonyl)-5-methoxy-1 <i>H</i> -indol-2-yl]ethanone
8	C	VII	9	[1-(furan-2-carbonyl)-5-methoxy-2-methyl-1 <i>H</i> -indol-3-yl]acetic acid
9	C	VIII	9	[5-methoxy-2-methyl-1-(thiophene-2-carbonyl)-1 <i>H</i> -indol-3-yl]acetic acid
10	A	VII	9	[5-bromo-1-(furan-2-carbonyl)-2-methyl-1 <i>H</i> -indol-3-yl]acetic acid
11	C	III	10	3-[1-(4-bromobenzoyl)-5-methoxy-2-methyl-1 <i>H</i> -indol-3-yl]propionic acid
12	C	III	14	4-[1-(4-bromobenzoyl)-5-methoxy-2-methyl-1 <i>H</i> -indol-3-yl]butyric acid
13	C	IV	10	3-[1-(biphenyl-4-carbonyl)-5-methoxy-2-methyl-1 <i>H</i> -indol-3-yl]propionic acid
14	C	VI	10	3-[5-methoxy-2-methyl-1-(pyridine-2-carbonyl)-1 <i>H</i> -indol-3-yl]propionic acid
15	C	VI	14	4-[5-methoxy-2-methyl-1-(pyridine-2-carbonyl)-1 <i>H</i> -indol-3-yl]butyric acid
16	F	I	1	9-(4-chlorobenzoyl)-6,7,8,9-tetrahydro-5 <i>H</i> -carbazole-3-sulfonic acid
17	F	I	4	1-(4-chlorobenzoyl)-3-ethyl-2-methyl-1 <i>H</i> -indole-5-sulfonic acid
18	F	I	5	5-(4-chlorobenzoyl)-2-methyl-2,3,4,5-tetrahydro-1 <i>H</i> -pyrido[4,3- <i>b</i>]indole-8-sulfonic acid
19	F	I	6	9-(4-chlorobenzoyl)-1,2,4,9-tetrahydro-3-thia-9-aza-fluorene-6-sulfonic acid
20	F	I	7	5-(4-chlorobenzoyl)-6,7,8,9,10,11-hexahydro-5 <i>H</i> -cycloocta[<i>b</i>]indole-2-sulfonic acid
21	F	I	11	1-(4-chlorobenzoyl)-3-decyl-2-methyl-1 <i>H</i> -indole-5-sulfonic acid
22	F	I	12	3-benzyl-1-(4-chlorobenzoyl)-2-methyl-1 <i>H</i> -indole-5-sulfonic acid
23	F	I	14	4-[1-(4-chlorobenzoyl)-2-methyl-5-sulfo-1 <i>H</i> -indol-3-yl]butyric acid
24	F	I	14Me	4-[1-(4-chlorobenzoyl)-2-methyl-5-sulfo-1 <i>H</i> -indol-3-yl]butyric acid methyl ester
25	F	I	15	2-benzoyl-5-(4-chlorobenzoyl)-2,3,4,5-tetrahydro-1 <i>H</i> -pyrido[4,3- <i>b</i>]indole-8-sulfonic acid
26	F	I	16	1-(4-chlorobenzoyl)-3-(4-hydroxybenzyl)-2-methyl-1 <i>H</i> -indole-5-sulfonic acid
27	E	I	10	3-[1-(4-chlorobenzoyl)-5-methoxy-2-methyl-1 <i>H</i> -indol-3-yl]propionic acid
28	E	I	14	4-[1-(4-chlorobenzoyl)-2,5-dimethyl-1 <i>H</i> -indol-3-yl]butyric acid
29	F	VII	1	9-(furan-2-carbonyl)-6,7,8,9-tetrahydro-5 <i>H</i> -carbazole-3-sulfonic acid
30	F	VII	4	3-ethyl-1-(furan-2-carbonyl)-2-methyl-1 <i>H</i> -indole-5-sulfonic acid
31	F	VII	6	9-(furan-2-carbonyl)-1,2,4,9-tetrahydro-3-thia-9-azafluorene-6-sulfonic acid
32	F	VII	10	3-[1-(furan-2-carbonyl)-2-methyl-5-sulfo-1 <i>H</i> -indol-3-yl]propionic acid
33	F	VII	10Me	3-[1-(furan-2-carbonyl)-2-methyl-5-sulfo-1 <i>H</i> -indol-3-yl]propionic acid methyl ester
34	F	VII	11	3-decyl-1-(furan-2-carbonyl)-2-methyl-1 <i>H</i> -indole-5-sulfonic acid
35	F	VII	12	3-benzyl-1-(furan-2-carbonyl)-2-methyl-1 <i>H</i> -indole-5-sulfonic acid
36	F	VII	14	4-[1-(furan-2-carbonyl)-2-methyl-5-sulfo-1 <i>H</i> -indol-3-yl]butyric acid
37	F	VII	14Me	4-[1-(furan-2-carbonyl)-2-methyl-5-sulfo-1 <i>H</i> -indol-3-yl]butyric acid methyl ester
38	F	VII	15	2-benzoyl-5-(furan-2-carbonyl)-2,3,4,5-tetrahydro-1 <i>H</i> -pyrido[4,3- <i>b</i>]indole-8-sulfonic acid
39	C	I	10	3-[1-(4-chlorobenzoyl)-5-methoxy-2-methyl-1 <i>H</i> -indol-3-yl]propionic acid
40	C	I	14	4-[1-(4-chlorobenzoyl)-5-methoxy-2-methyl-1 <i>H</i> -indol-3-yl]butyric acid
41	G	I	1	9-(4-chlorobenzoyl)-6,7,8,9-tetrahydro-5 <i>H</i> -carbazole-3-carboxylic acid
42	G	I	6	9-(4-chlorobenzoyl)-1,2,4,9-tetrahydro-3-thia-9-azafluorene-6-carboxylic acid
43	G	I	11	1-(4-chlorobenzoyl)-3-decyl-2-methyl-1 <i>H</i> -indole-5-carboxylic acid
44	G	I	14	3-(3-carboxypropyl)-1-(4-chlorobenzoyl)-2-methyl-1 <i>H</i> -indole-5-carboxylic acid
45	F	IV	1	9-(biphenyl-4-carbonyl)-6,7,8,9-tetrahydro-5 <i>H</i> -carbazole-3-sulfonic acid
46	F	IV	5	5-(biphenyl-4-carbonyl)-2-methyl-2,3,4,5-tetrahydro-1 <i>H</i> -pyrido[4,3- <i>b</i>]indole-8-sulfonic acid
47	F	IV	6	9-(biphenyl-4-carbonyl)-1,2,4,9-tetrahydro-3-thia-9-azafluorene-6-sulfonic acid
48	F	IV	11	1-(biphenyl-4-carbonyl)-3-decyl-2-methyl-1 <i>H</i> -indole-5-sulfonic acid
49	F	IV	12	3-benzyl-1-(biphenyl-4-carbonyl)-2-methyl-1 <i>H</i> -indole-5-sulfonic acid
50	F	IV	14	4-[1-(biphenyl-4-carbonyl)-2-methyl-5-sulfo-1 <i>H</i> -indol-3-yl]butyric acid
51	F	IV	15	2-benzoyl-5-(biphenyl-4-carbonyl)-2,3,4,5-tetrahydro-1 <i>H</i> -pyrido[4,3- <i>b</i>]indole-8-sulfonic acid
52	F	IV	16	1-(biphenyl-4-carbonyl)-3-(4-hydroxybenzyl)-2-methyl-1 <i>H</i> -indole-5-sulfonic acid
53	F	VI	1	9-(pyridine-2-carbonyl)-6,7,8,9-tetrahydro-5 <i>H</i> -carbazole-3-sulfonic acid
54	F	VI	6	9-(pyridine-2-carbonyl)-1,2,4,9-tetrahydro-3-thia-9-azafluorene-6-sulfonic acid
55	C	VIII	10Et	3-[5-methoxy-2-methyl-1-(thiophene-2-carbonyl)-1 <i>H</i> -indol-3-yl]propionic acid ethyl ester
56	C	VIII	14	4-[5-methoxy-2-methyl-1-(thiophene-2-carbonyl)-1 <i>H</i> -indol-3-yl]butyric acid
57	C	IX	9	[1-(4-(dimethylamino)benzoyl)-5-methoxy-2-methyl-1 <i>H</i> -indol-3-yl]acetic acid
58	C	IX	10	3-[1-(4-(dimethylamino)benzoyl)-5-methoxy-2-methyl-1 <i>H</i> -indol-3-yl]propionic acid
59	C	IX	14	4-[1-(4-(dimethylamino)benzoyl)-5-methoxy-2-methyl-1 <i>H</i> -indol-3-yl]butyric acid
60	C	IX	14Et	4-[1-(4-(dimethylamino)benzoyl)-5-methoxy-2-methyl-1 <i>H</i> -indol-3-yl]butyric acid ethyl ester

Evaluation of Cytotoxicity. The human glioblastoma cell line T98G, which is known to express MRP-1,¹⁴ was chosen for the biological assays. MRP expression was analyzed by reverse transcription and PCR. The MRP transcript of the expected size was detected in T98G cells of the same passaging step as that used in the further assays (Figure 3A).¹⁴ Next we confirmed the translation of the MRP transcript. The clear band at the approximate size of the MRP-1 protein in the Western blot showed that the protein is present in T98G cells (Figure 3B). Not surprisingly, the relative amount of the membrane protein MRP-1 was higher in the total

lysate, which comprises the membrane fraction, as compared to the soluble fraction of the cells. Into a 96-well plate, 10⁴ cells/well were seeded. During the initial phase of assay optimization, concentrations of indomethacin analogues were between 1.25 and 160 μM and doxorubicin concentrations were between 0.08 and 40 μM. In the final assay indomethacin analogues were used at 5–10 μM and doxorubicin at 0.1–1.0 μM. The final dimethyl sulfoxide (DMSO) concentration over a period of 4 days did not exceed 0.5%. As tested in a control experiment, this DMSO concentration is not toxic for T98G cells (not shown). Figure 4 shows the cell

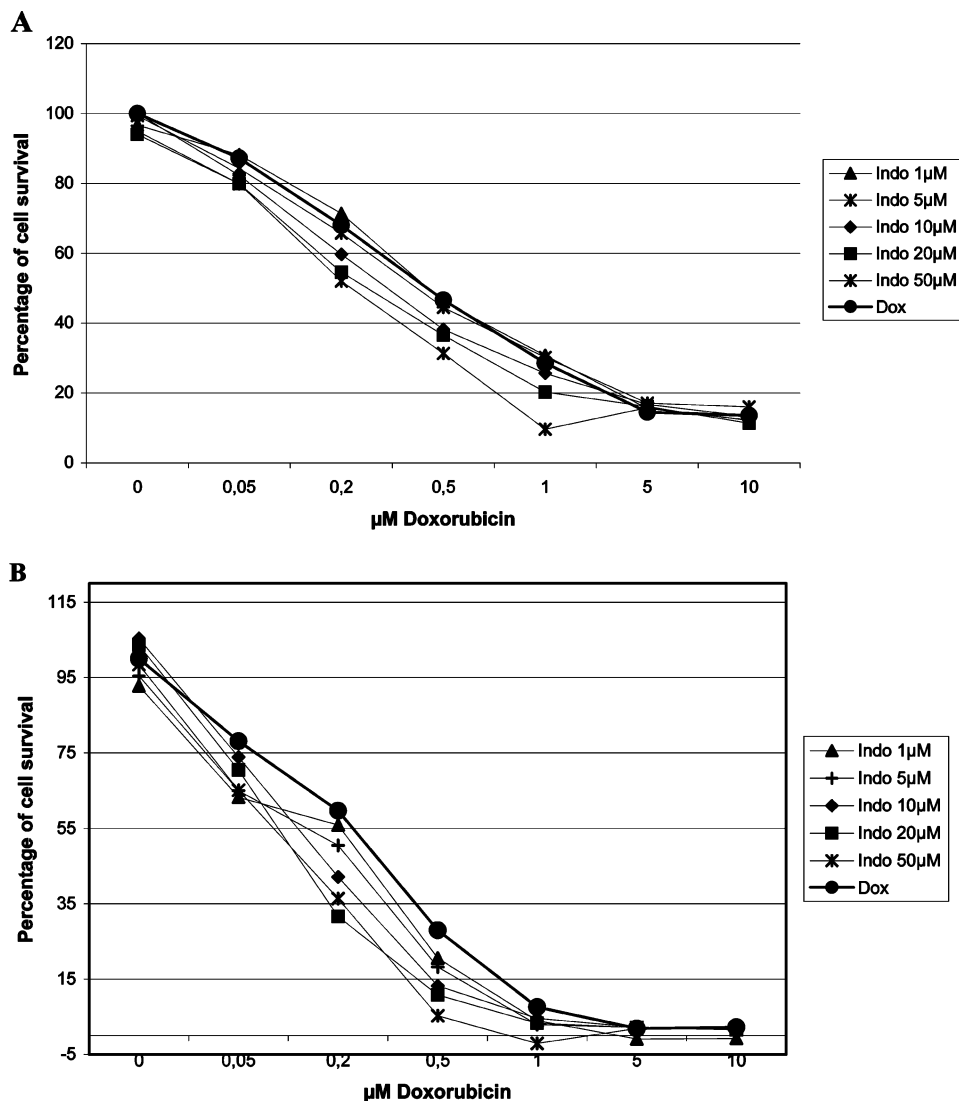


Figure 4. Indomethacin sensitizes T98G human malignant glioma cells to doxorubicin cytotoxicity. T98G cells were pretreated with indomethacin [$c(\text{indomethacin}) = 1\text{--}50\ \mu\text{M}$] for 2 h and then cotreated with doxorubicin [$c(\text{doxorubicin}) = 0\text{--}10\ \mu\text{M}$] for (A) 3 or (B) 4 days. Survival was measured by crystal violet staining as described in Materials and Methods. Data are expressed as the mean percentage of survival (SD < 10%; $n = 3$).

survival rate at six different indomethacin concentrations in dependence of the doxorubicin concentration after 3 and 4 days. The results show that the signal-to-noise ratio is significant after 4 days. Thus, the following assays to measure the combined toxicity of the potential MRP-1 inhibitors and the cytostatic drug doxorubicin were performed after an incubation time of 4 days.

In a preliminary experiment we tested the potentially inhibiting effects of 60 different indoles at a concentration of $10\ \mu\text{M}$ without or with 0.2, 0.5, or $1\ \mu\text{M}$ doxorubicin. The results showed the influence of the indole compounds on the cytotoxicity of doxorubicin (Figure 5). On the basis of these results, we classified the derivatives into three groups (Table 3). Group **a** comprises 24 molecules, which neither increased the cytotoxic effects of doxorubicin nor had any other effect on cell survival under the applied conditions. In group **b** the substances were classified, which increased doxorubicin induced cell mortality. The effect of these 23 compounds was at least 10% weaker than the effect shown with indomethacin. Group **c** comprises nine

molecules, which increased the cytotoxicity of doxorubicin at the same or at an even 13% higher level than indomethacin itself. Finally category **d** comprises toxic substances, which caused an increased general cell mortality at $10\ \mu\text{M}$ even in the absence of doxorubicin. The incubation with the four agents of this group decreased the cell number by at least 30% compared to the untreated control. Such toxic effects circumvent the differentiation between the toxicity of the compound and a potential inhibition of MRP-1. Thus, the compounds of group **d** could not be evaluated in the assay.

The classification of all 60 compounds according to these criteria allowed first important conclusions about the structure–function relationships (Table 3). The replacement of the methoxy moiety at the hydrazine building block **C** (Figure 2) by bromine (**A**) or by sulfonic acid (**F**) leads to the loss of activity. Also fluoryl and nicotinic acid chloride building blocks (**VII** and **X**) led to inactive indoles. All tested esters showed lower activities compared to the free acid and often showed an increased toxicity. One possible explanation for lower activity of the esters could be a direct interaction

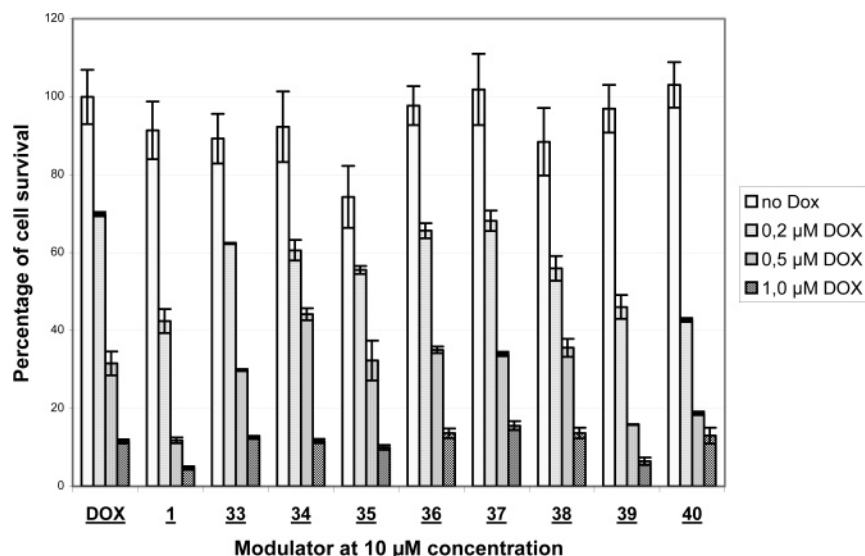


Figure 5. Exemplified results of preliminary experiments performed at a constant concentration to identify potentially interesting compounds. T98G cells were pretreated with indomethacin [$c(\text{indomethacin}) = 10 \mu\text{M}$] for 2 h and then cotreated with doxorubicin [$c(\text{doxorubicin}) = 0\text{--}1.0 \mu\text{M}$] for 4 days. Survival was measured by crystal violet staining as described in Materials and Methods. Data shown are the mean percentage \pm SD for a minimum of three experiments.

Table 3. Summary of the Cytotoxicity Assay Results and Classification of All Nonsteroidal Antiinflammatory Compounds According Their Effects at $c(\text{compound}) = 10 \mu\text{M}$

classification	compound no.
(a) inactive ^a	6, 8, 10, 14, 16, 17, 19, 20, 21, 22, 24, 29, 30, 31, 32, 33, 34, 36, 37, 38, 46, 49, 50, 52
(b) active ^b	1, 2, 4, 5, 7, 9, 13, 15, 25, 26, 43, 44, 45, 47, 51, 53, 54, 56, 57, 58, 59, 60
(c) very active ^c	3, 11, 12, 27, 28, 39, 40, 41, 42
(d) toxic ^d	18, 23, 35, 48, 55

^a Inactive compounds had no synergistic effect on the doxorubicin-induced cell death at $c(\text{doxorubicin}) = 0.1 \mu\text{M}$. ^b Active compounds increased doxorubicin-induced cell mortality at least 10% lower than indomethacin at $c(\text{doxorubicin}) = 0.1 \mu\text{M}$. ^c Very active compounds increased doxorubicin-induced cell mortality to a similar or up to 13% higher extent than indomethacin at $c(\text{doxorubicin}) = 0.1 \mu\text{M}$. The general structures of these compounds are given in Figure 8. The detailed assay results of all compounds of category **c** are given in the Supporting Information. ^d Toxic compounds increased general cell mortality even in the absence of doxorubicin. At the NSAID concentrations of $10 \mu\text{M}$ the cell survival was $<70\%$. Therefore these compounds were not evaluated any further.

between the carboxylic acid and MRP-1. This model is supported by the fact that MRP-1 shows a preference for hydrophilic compounds and transports amphiphilic organic anions.^{12, 5}

The nine active compounds categorized in group **c** (Figure 6) were analyzed in further detail. These analyses were performed with $5 \mu\text{M}$ indole concentration and 0.1, 0.2, 0.5, and $0.8 \mu\text{M}$ doxorubicin concentration. All measurements were done in triplicate. In these experiments the seven compounds **3**, **27**, **28**, **39**, **40**, **41**, and **42** induced a high increase in doxorubicin toxicity. All these compounds showed an inhibition of MRP-1 at a level similar to that of indomethacin. Remarkably, derivatives **11** and **12** showed an even higher inhibition compared to indomethacin (Table 4). On the basis of the data shown in Table 4, the cell mortalities induced by indomethacin and analogues **11** and **12** in a combined application with doxorubicin were correlated to the cell mortality of doxorubicin alone. Figure 7 illustrates, e.g., that indomethacin (at $5 \mu\text{M}$) in combination with doxorubicin (at $0.1 \mu\text{M}$) increases the cell death in the described assay conditions compared to doxorubicin alone up to 9% and the cell mortality is amplified to 22% when compound **11** is used in the same assay system. This 2.4-fold increased cytotoxicity induced by indomethacin analogues **11** demonstrates the potential of the combinatorial chemistry approach with the in-

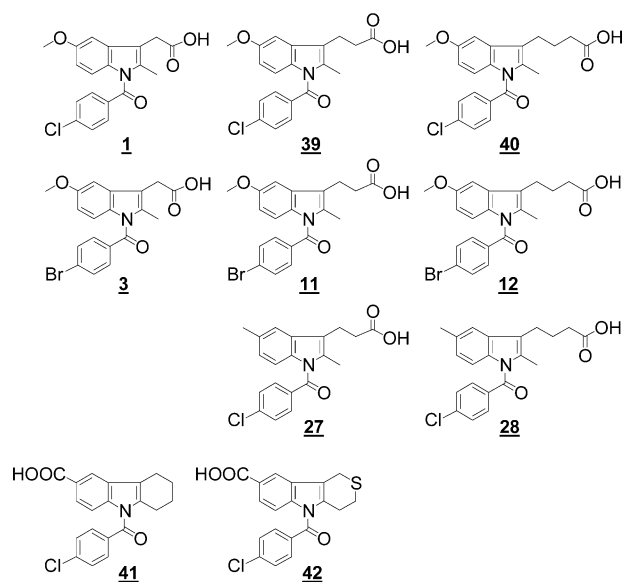


Figure 6. Structures of the nine active indomethacin analogues (category **c**, Table 3).

domethacin core structure. Due to the reason that in some cancer cell lines the IC_{50} of doxorubicin is below $0.1 \mu\text{M}$, the synergistic effect of indomethacin especially in this low concentration range is of particular impor-

Table 4. Demonstration of a Synergistic Combination of Selected Nonsteroidal Antiinflammatory Drugs (NSAIDs) with Doxorubicin as the Chemotherapeutic Drug in T98G Cells^a

	no NSAID	indomethacin (5 μ M)	11 (5 μ M)	12 (5 μ M)
no DOX	100.0 \pm 4.3	100.9 \pm 1.3	95.5 \pm 3.3	95.2 \pm 2.1
0.1 μ M DOX	75.8 \pm 4.9	69.3 \pm 0.3	59.0 \pm 2.6	63.6 \pm 2.3
0.2 μ M DOX	71.4 \pm 2.2	56.6 \pm 3.2	48.6 \pm 1.9	53.7 \pm 3.9
0.5 μ M DOX	37.2 \pm 1.0	18.7 \pm 2.1	11.6 \pm 2.6	16.9 \pm 2.3

^a Data are expressed as percentage cell survival \pm standard deviation for a minimum of three determinations. The NSAID concentrations were nontoxic (cell survival > 95%) in all cases.

tance.¹⁰ Especially at this clinically relevant low doxorubicin concentration of 0.1 μ M the two novel compounds showed significant effects and no general toxicity in the absence of doxorubicin.

The goal of our investigation was to identify novel compounds which are more potent inhibitors of MDR observed in the presence of the cytostatic therapeutic doxorubicin. Overall we analyzed a library of 60 indomethacin analogues in a combined toxicity cell biological assay. The results revealed nine very active compounds. Compound **11** displayed an increase of the doxorubicin-induced cytotoxicity by a factor of 2.4 and compound **12** by a factor of 1.7. Thus, structure **11** represents an attractive starting point for the development of potent MRP-1 inhibitors.

All compounds classified as very active showed a high structural homology to indomethacin (Figure 8). The extension of the alkyl chain by a methylene group in **11** led to an activity increase in comparison to indomethacin. However, the additional CH₂ group in **12** has no further effect. Remarkably, only the use of 4-halogen-substituted benzoyl building blocks led to active compounds. The most active compounds **11** and **12** carry a bromine substituent. As molecules **27** and **28** demonstrate, the methoxy group of indomethacin can also be substituted by a methyl group without complete loss of activity. On first glance the high activities of **41** and **42** seem surprising, because these molecules do not have the 3-indole acetic acid motif of indomethacin. However, closer inspection of the structure shows that the acid function of **41** is in comparable distance to the central pyrrole as in **11** (see Figure 9). The free carboxylic acid in **41** is bound to the aromatic six-membered ring of the indole, which carries a nonsubstituted nonpolar ring as an equivalent to the methoxyphenyl motif in **11**. This structural relationship indicates a rigid donor acceptor relation between the free acid and the *N*-benzoyl motif and amino acids of MRP-1, which may be crucial for MRP-1 activity.

In the present report we have described a synthesis procedure and SAR studies based on the known MRP-1 inhibitor **1**. As a result, two novel and potent MRP-1 modulators with no cytotoxicity (cell survival > 95% at $C_{\text{modulator}} < 10 \mu\text{M}$) were identified. We have demonstrated that these indomethacin analogues have the ability to potentiate the toxicity of the chemotherapeutic agent doxorubicin, and they are an attractive starting point for further development of MRP-1 inhibitors. In some cancers, where drug resistance is a result of MRP-1 overexpression, this synergistic effect of NSAIDs with chemotherapeutic agents potentially improves existing treatments for cancer.

Experimental Section

General Methods for Chemical Synthesis. Materials.

Unless otherwise noted, reagents were purchased from Acros Chimica, Fluka, Sigma, and Aldrich and used without further purification. LC-MS was performed on the 1100 series from Hewlett-Packard with a VP 50/10 Nucleosil C18PPN column (Macherey-Nagel) and a Finnigan LCQ ESI spectrometer with a gradient: 90/10 (v/v) H₂O/acetonitrile (0.1% trifluoroacetic acid) to 10/90 (v/v) in 30 min; flow, 1 mL/min. Preparative HPLC was conducted by using Pro Star 215/Varian HPLC with a VP 250/21 Nucleosil C18PPN column (Macherey-Nagel) and a gradient: 90/10 (v/v) H₂O/acetonitrile (0.1% trifluoroacetic acid) to 10/90 (v/v) in 30 min; flow, 20 mL/min. Nuclear magnetic resonance (NMR) spectra were recorded on a Varian Mercury 400 (400 MHz ¹H NMR; 100.6 MHz ¹³C NMR). ¹H NMR spectra are tabulated in the following order: chemical shifts calculated with reference to solvent standards based on tetramethylsilane, multiplicity (s, singlet; d, doublet; t, triplet; q, quartet; m, multiplet), coupling constants in Hz, and number of protons. The 70 eV electron ionization (EI) high-resolution mass spectra (HR-MS) were recorded on Finnigan MAT MS 70 spectrometer.

General Procedure for Hydrazone Formation. The aldehyde resin (0.5 g, 0.55 mmol) was dried in high vacuum overnight and suspended in 5 mL of dichloroethane (DCE). To this suspension, 2.75 mmol (5 equiv) of hydrazine hydrochloride and 194 μ L (6 equiv) of triethylamine (NEt₃) were added under argon atmosphere. The mixture was shaken at 45 °C overnight. After cooling the resin was filtered and washed three times with each 5 mL of *N,N*-dimethylformamide (DMF), 90/10 (v/v) DMF/H₂O, DMF, dichloromethane, ethyl acetate, and methanol.

General Procedure for Hydrazone Acylation. The hydrazone resin (0.5 g, 0.45 mmol) was dried in high vacuum overnight and suspended in 5 mL of pyridine. To the mixture 1.35 mmol (3 equiv) of acid chloride was added under argon. The mixture was shaken at 80 °C overnight. After cooling the resin was filtered and washed three times with *N,N*-dimethylformamide (DMF), 90/10 (v/v) DMF/H₂O, DMF, dichloromethane, ethyl acetate, and methanol.

General Procedure for Cleavage and Indole Rearrangement. The acylated hydrazone resin (150 mg, 0.11 mmol) was suspended in 6 mL of DCE/TFA (1/1). The corresponding ketone (10 equiv) was added, and the mixture was heated for 15 min to 2 h at 70 °C. After cooling the mixture was quenched with methanol and the resin was filtered and washed with 5 mL of dichloromethane, methanol, ethyl acetate, and methanol. The filtrate was evaporated to dryness, and the crude product was purified by preparative HPLC.

Analytical Data for Selected Compounds. (a) [1-(4-Bromobenzoyl)-5-methoxy-2-methyl-1H-indol-3-yl]acetic Acid (3**; C-III-9).** White solid; yield 57%; HPLC purity > 99% (215 nm); mp 151 °C. ¹H NMR (400 MHz, CD₃OD): δ 7.73 (d, ³J = 8.2 Hz, 2 H, arom CH), 7.60 (d, ³J = 8.2 Hz, 2 H, arom CH), 7.00 (d, ⁴J = 2.5 Hz, 1 H, arom CH), 6.91 (d, ³J = 8.6 Hz, 1 H, arom CH), 6.67 (dd, ³J = 8.6 Hz, ⁴J = 2.5 Hz, 1 H, arom CH), 3.80 (s, 3 H, OCH₃), 3.69 (s, 2 H, CH₂), 2.31 (s, 3 H, CH₃). MS (ESI): 400.0 [M - H]⁻. HR-MS (FAB, *m/z*). Calcd for C₁₉H₁₅BrNO₄ [M - H]⁻: 400.0185. Found: 400.0181.

(b) 3-[1-(4-Bromobenzoyl)-5-methoxy-2-methyl-1H-indol-3-yl]propionic Acid (11**; C-III-10).** White solid; yield 25%; HPLC purity > 99% (215 nm); mp 210 °C. ¹H NMR (400 MHz, CD₃OD): δ 7.73 (d, ³J = 8.2 Hz, 2 H, arom CH), 7.60 (d, ³J = 8.2 Hz, 2 H, arom CH), 7.00 (d, ⁴J = 2.5 Hz, 1 H, arom CH), 6.91 (d, ³J = 8.6 Hz, 1 H, arom CH), 6.67 (dd, ³J = 8.6 Hz, ⁴J = 2.5 Hz, 1 H, arom CH), 3.80 (s, 3 H, OCH₃), 2.81 (t, ³J = 7.6 Hz, 2 H, CH₂), 2.49 (t, ³J = 7.6 Hz, 2 H, CH₂), 2.29 (s, 3 H, CH₃). MS (ESI): 414.39; 416.36 [M - H]⁻. HR-MS (FAB, *m/z*). Calcd for C₂₀H₁₇BrNO₄ [M - H]⁻: 414.0341. Found: 414.0346.

(c) 4-[1-(4-Bromobenzoyl)-5-methoxy-2-methyl-1H-indol-3-yl]butyric Acid (12**; C-III-14).** Green solid; yield 71%; HPLC purity > 99% (215 nm); mp 210 °C. ¹H NMR (400 MHz, CD₃OD): δ 7.70 (d, ³J = 8.2 Hz, 2 H, arom CH), 7.57 (d, ³J =

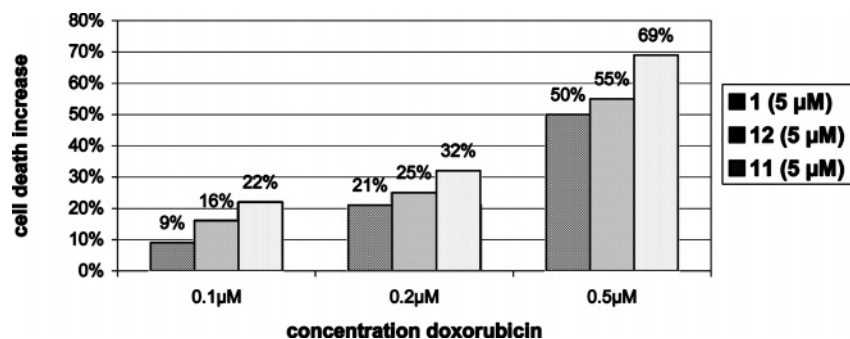


Figure 7. Demonstration of cell death increase in a combined application of doxorubicin and NSAIDs. The doxorubicin-induced cell death is correlated to the cell death caused by the addition of NSAIDs. The chart illustrates the activities of the compounds indomethacin, **11**, and **12** in comparison to doxorubicin.

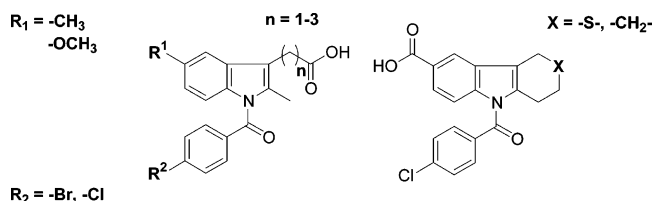


Figure 8. General structures of the nine very active indole derivatives (category **c**, Table 3).

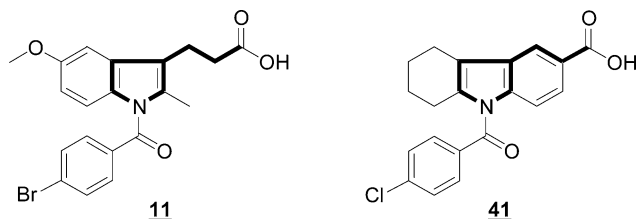


Figure 9. Comparative representation of compounds **11** and **41** to demonstrate their structural similarity.

8.2 Hz, 2 H, arom CH), 7.08 (d, $^4J = 2.5$ Hz, 1 H, arom CH), 6.23 (d, $^3J = 8.6$ Hz, 1 H, arom CH), 6.65 (dd, $^3J = 8.6$ Hz, $^4J = 2.5$ Hz, 1 H, arom CH), 3.81 (s, 3 H, OCH₃), 2.73 (t, $^3J = 7.00$ Hz, 2 H, CH₂), 2.37 (t, $^3J = 7.00$ Hz, 2 H, CH₂), 2.26 (s, 3 H, CH₃), 1.91 (q, $^3J = 7.00$ Hz, 2 H, CH₂). MS (ESI): 430.23; 428.23 [M - H]⁻. HR-MS (FAB, m/z). Calcd for C₂₁H₁₉BrNO₄ [M - H]⁻: 428.0497. Found: 428.0505.

(d) **3-[1-(4-Chlorobenzoyl)-2,5-dimethyl-1H-indol-3-yl]propionic Acid (27; E-I-10)**. White solid; yield 23%; HPLC purity > 99% (215 nm). LC-MS (ESI): 354.64 [M - H]⁻. $R_t = 11.41$ min; C₂₀H₁₈ClNO₃, 355.8146 g/mol.

(e) **4-[1-(4-Chlorobenzoyl)-2,5-dimethyl-1H-indol-3-yl]butyric Acid (28; E-I-14)**. White solid; yield 25%; HPLC purity > 99% (215 nm). LC-MS: 368.28 [M - H]⁻. $R_t = 12.03$ min; C₂₁H₂₀ClNO₃, 369.84 g/mol.

(f) **3-[1-(4-Chlorobenzoyl)-5-methoxy-2-methyl-1H-indol-3-yl]propionic Acid (39; C-I-10)**. White solid; yield 39%; HPLC purity > 99% (215 nm). LC-MS: 370.14 [M - H]⁻. $R_t = 5.49$ min; C₂₁H₂₀ClNO₃, 371.8140 g/mol.

(g) **4-[1-(4-Chlorobenzoyl)-5-methoxy-2-methyl-1H-indol-3-yl]butyric Acid (40; C-I-14)**. White solid; yield 46%; HPLC purity > 99% (215 nm); mp 105 °C. ¹H NMR (400 MHz, CD₃OD): δ 7.64 (d, $^3J = 8.2$ Hz, 2 H, arom CH), 7.54 (d, $^3J = 8.2$ Hz, 2 H, arom CH), 7.03 (d, $^4J = 2.5$ Hz, 1 H, arom CH), 6.2 (d, $^3J = 8.6$ Hz, 1 H, arom CH), 6.65 (dd, $^3J = 8.6$ Hz, $^4J = 2.5$ Hz, 1 H, arom CH), 3.81 (s, 3 H, OCH₃), 2.73 (t, $^3J = 7.00$ Hz, 2 H, CH₂), 2.37 (t, $^3J = 7.00$ Hz, 2 H, CH₂), 2.26 (s, 3 H, CH₃), 1.91 (q, $^3J = 7.00$ Hz, 2 H, CH₂). MS (ESI): 384.18 [M - H]⁻. HR-MS (FAB, m/z). Calcd for C₂₁H₁₉ClNO₄ [M - H]⁻: 384.1002. Found: 384.1013.

(h) **9-(4-Chlorobenzoyl)-6,7,8,9-tetrahydro-5H-carbazole-3-carboxylic Acid (41; G-I-1)**. White solid; yield 26%; HPLC purity > 99% (215 nm); mp 254–255 °C. ¹H NMR (400 MHz, CDCl₃): δ 8.12 (d, $^4J = 2.0$ Hz, 1 H, arom CH), 7.78 (dd,

$^3J = 9$ Hz, $^4J = 2.0$ Hz, 1 H, arom CH), 7.66 (d, $^3J = 8.6$ Hz, 2 H, arom CH), 7.54 (d, $^3J = 8.6$ Hz, 2 H, arom CH), 7.24 (d, $^3J = 9$ Hz, 1 H, arom CH), 2.73 (t, $^3J = 6$ Hz, 2 H, CH₂), 2.57 (t, $^3J = 6$ Hz, 2 H, CH₂), 1.82–2.03 (m, 4 H, CH₂). ¹³C NMR (100.6 MHz, CDCl₃): δ 210.19 (C=O), 179.37 (C=O), 139.26 (C_q), 137.59 (C_q), 137.29 (C_q), 139.97 (C_q), 131.02 (arom CH), 129.15 (arom CH), 127.35 (C_q), 125.12 (C_q), 124.83 (arom CH), 120.20 (arom CH), 118.28 (C_q), 114.00 (arom CH), 25.77 (CH₂), 23.58 (CH₂), 22.33 (CH₂), 21.05 (CH₂). MS (ESI): 352.16 [M - H]⁻. HR-MS (FAB, m/z): Calcd for C₂₀H₁₅ClNO₃ [M - H]⁻: 352.0741. Found: 352.0767.

(i) **9-(4-Chlorobenzoyl)-1,2,4,9-tetrahydro-3-thia-9-azafluorene-6-carboxylic Acid (42; G-I-11)**. White solid; yield 6%; HPLC purity > 99% (215 nm). LC-MS: 370.11 [M - H]⁻. $R_t = 5.57$ min; C₁₉H₁₄ClNO₃S, 371.8381 g/mol.

Reverse Transcription PCR. The expression of the MRP gene was controlled by reverse-transcription PCR (RT-PCR) of the MRP transcript. RNA was purified from T89G cells by standard methods (RNeasy Mini Kit, Qiagen). For PCR the purified RNA was reverse-transcribed into cDNA using Omniscript Reverse Transcriptase (Qiagen). The following primers were used for the PCR of the MRP cDNA:¹⁴ MRP sense, 5'-CGTGTACTCCAACGCTGAC-3'; MRP antisense, 5'-CTGGACCGTGACGCCCGTGAC-3'. The template was denatured for 5 min at 95 °C, and the PCR was carried out for 35 cycles, which included 45 s at 95 °C, 45 s at 55 °C, and 60 s at 72 °C. The MRP product was expected to be of a length of 326 bp. For positive control, β-actin was directly amplified by OneStep RT-PCR (Qiagen) from RNA. The used primers were as follows: β-actin sense 5'-GCGGGATCCTCGACAACGGCTCGGCAT-3'; β-actin antisense 5'-GCGGTGACGGATCTTCATGAGGTAGTCAG-3'. The RT-PCR program was as follows: 30 min at 50 °C, 15 min at 95 °C, and 35 cycles at 30 s at 94 °C, 30 s at 60 °C, and 60 s at 72 °C. The resulting β-actin fragment was expected to be of a length of 628 bp. The PCR result was controlled by electrophoresis in 2% agarose gels using a 100 bp ladder marker (Fermentas). Gels were stained by ethidium bromide.

Western Blot. The T98G cells were analyzed for the presence of the MRP-1 protein. Subconfluent cells were harvested and resuspended in PBS including a mix of protease inhibitors (Complete from Roche). Cells were lysed on ice by ultrasound sonication. The total lysate was centrifuged for 10 min at 13 000 rpm. The resulting supernatant and the total lysate were adjusted to equal protein concentrations as determined by Bradford protein concentration determination. A 35 mg amount of total protein of each sample was separated by SDS-PAGE on a 7.5% gel and blotted on a PVDF membrane (Amersham). The membrane was blocked with blocking buffer (5% powdered milk, 0.1% Tween20 in PBS) for 2 h. The membrane was incubated with anti-MRP-1 antibody (QCRL-1 clone from Santa Cruz Biotechnology) at 1:100 dilution in blocking buffer overnight. Next the membrane was incubated with HRPO-coupled anti-mouse-antibody (Amersham Biosciences) at 1:20 000 dilution in blocking buffer for 1 h at room temperature. The membrane was developed using

the ECL Plus Western blot detection system (Amersham Biosciences).

Cell Line and Cytotoxicity Assay. The human glioblastoma cell line T98G was purchased from American Type Culture Collection (Rockville, MD). Cells were cultured under standard conditions. Cytotoxicity was evaluated by measuring the metabolic activity of the cells by using the 3-(4,5-dimethylthiazol-2-yl)-2,5-diphenyltetrazolium bromide (MTT) assay.¹⁸ Briefly, the T98G cells were seeded at 10⁴ cells/well in 96-well plates, adhered for 24 h, and exposed to 10 μ M of the drugs for 4 days. A 100 μ L aliquot of the cultured medium was removed, and the cells were treated with 20 μ L of PBS containing 5 mg/mL MTT (Sigma). After incubation at 37 $^{\circ}$ C in a humidified air atmosphere (7.5% CO₂) for 2 h, 150 μ L of 2-propanol containing 0.04 mol/L HCl were added to each well to dissolve the formazan crystals produced from the reduction of MTT by viable cell. After incubation of 45 min and trituration the absorbance from each well was measured at 620 nm. The results were expressed as percentages relative to control cells. The experiments were performed in triplicates and repeated at least three times.

Acknowledgment. This research was supported by the Max Planck Gesellschaft and the Fonds der Chemischen Industrie. C.R. is grateful to the Landesgraduierten Stiftung Baden-Württemberg for financial support. We thank Anette Langerak for excellent technical assistance.

Supporting Information Available: Biological data concerning the effect of compounds **3**, **11**, **12**, **27**, **28**, and **39–42** on the modulation of multidrug resistance in T98G cells and analytical data for 23 selected compounds of the indomethacin-derived library are available. This material is available free of charge via the Internet at <http://pubs.acs.org>.

References

- Chen, C.; Chin, J. E.; Ueda, K.; Clark, D. R.; Pastan, I.; Gottesman, M. M.; Roninson, I. B. Internal Duplication and Homology with Bacterial Transport Proteins in the *mdr-1* (*P*-Glycoprotein) Gene from Multidrug Resistant Human Cells. *Cell* **1986**, *47*, 381–389.
- Borst, P.; Evers, R.; Kool, M.; Wijnholds, J. J. A Family of Drug Transporters: The Multidrug Resistance-Associated Proteins. *Natl. Cancer Inst.* **2000**, *92*, 1295–1302.
- Cole, S. P. C.; Bhardwaj, G.; Gerlach, J. H.; Mackie, J. E.; Grant, C. E.; Almquist, K. C.; Stewart, A. J.; Kurz, E. U.; Duncan, A. M. V.; Deeley, R. G. Overexpression of a Transporter Gene in a Multidrug-Resistant Human Lung Cancer Cell Line. *Science* **1992**, *258*, 1650–1654.
- Ruh, G. D.; Gaughan, K. T.; Godwin, G.; Chan, A. J. Expression Pattern of MRP in Human Tissues and Adult Solid Tumor Cell Lines. *Natl. Cancer Inst.* **1995**, *87*, 1256–1258.
- Cole, S. P. C.; Sparks, K. E.; Fraser, K.; Loe, D. W.; Grant, C. E.; Wilson, G. M.; Deeley, R. G. Pharmacological Characterization of Multidrug Resistant MRP-Transfected Human Tumor Cells. *Cancer Res.* **1994**, *54*, 5902–5910.
- Bodo, A.; Bakos, E.; Szeri, F.; Varadi, A.; Sarkadi, B. The Role of Multidrug Transporters in Drug Availability Metabolism and Toxicity. *Toxicol. Lett.* **2003**, *140–141*, 133–143.
- Fisher, G. A.; Lum, B. L.; Hausdorff, J.; Sikic, B. I.; Pharmacological Considerations in the Modulation of Multidrug Resistance. *Eur. J. Cancer* **1996**, *32A*, 1082–1088.
- Gollapudi, S.; Thadepalli, F.; Kim, C. H. Difloxacin Reverses Multidrug Resistance in HL-60/AR Cells That Overexpress the Multidrug Resistance-Related Protein (MRP) Gene. *Oncol. Res.* **1995**, *7*, 231–225.
- Alberts, D. S.; Hixson, L.; Ahnen, D.; Bogert, C.; Einspahr, J.; Paranka, N.; Brendel, K.; Gross, P. H.; Pamukcu, R.; Burt, R. W. J. Do NSAIDs Exert Their Colon Cancer Chemoprevention Activities through the Inhibition of Mucosal Prostaglandin Synthetase? *Cell. Biochem.* **1994**, *S22*, 18–23.
- Duffy, C. P.; Elliott, C. J.; O'Connor, R. A.; Heenan, M. M.; Colye, S.; Ceary, I. M.; Kavanagh, K.; Verhaegen, S.; O'Loughlin, C. M.; NicAmhlaoibh, R.; Clynes, M. Enhancement of Chemotherapeutic Drug Toxicity to Human Tumour Cells in Vitro by a Subset of Nonsteroidal Antiinflammatory Drugs (NSAIDs). *Eur. J. Cancer* **1998**, *34*, 1250–1259.
- Draper, M. P.; Martell, R. L.; Levy, S. B. Indomethacin-Mediated Reversal of Multidrug Resistance and Murine Cell Lines Overexpressing MRP, but Not *p*-Glycoprotein. *Br. J. Cancer* **1997**, *75*, 810–815.
- Tønnessen, T. I.; Aas, A. T.; Sandvig, K.; Olsnes, S. Inhibition of Chloride/Bicarbonate Antiports in Monkey Kidney Cells (Vero) by Nonsteroidal Antiinflammatory Drugs. *Biochem. Pharmacol.* **1989**, *38*, 3583–3591.
- Touhey, S.; O'Connor, R.; Plunkett, S.; Maguire, A.; Clynes, M. Structure–Activity Relationship of Indomethacin Analogues for MRP-1, COX-1 and COX-2 Inhibition: Identification of Novel Chemotherapeutic Drug Resistance Modulators. *Eur. J. Cancer* **2002**, *38*, 1661–1670.
- Roller, A.; Bähr, O. R.; Streffer, J.; Winter, S.; Heneka, M.; Deininger, M.; Meyermann, R.; Naumann, U.; Gulbins, E.; Weller, M. Selective Potentiation of Drug Cytotoxicity by NSAID in Human Glioma Cells: The Role of COX-1 and MRP. *Biochem. Biophys. Res. Commun.* **1999**, *259*, 600–605.
- For Fischer indole syntheses on the solid support see: (a) Hutchins, S. M.; Chapman, K. T. Fischer Indole Synthesis on a Solid Support. *Tetrahedron Lett.* **1996**, *37*, 4869–4872. (b) Yang, L. Facile Cleavage of the Carbamate Linker of Hydroxymethyl Resin and Its Application in Syntheses Requiring Strongly Acidic Conditions. *Tetrahedron Lett.* **2000**, *41*, 6981–6984. (c) Cooper, L. C.; Chicchi, G. G.; Dinnell, K.; Elliott, J. M.; Hollingworth, G. J.; Kurtz, M. M.; Locker, K. L.; Morrison, D.; Shaw, D. E.; Tsao, K.-L.; Watt, A. P.; Williams, A. R.; Swain, C. J. 2-Aryl Indole NK₁ Receptor Antagonists: Optimisation of Indole Substitution. *Bioorg. Med. Chem. Lett.* **2001**, *11*, 1233–1236. (d) Tois, J.; Franzén, R.; Aitio, O.; Huikko, K.; Taskinen, J. Preparation of 5-Substituted 2-Carboxyindoles on Solid Support. *Tetrahedron Lett.* **2000**, *41*, 2443–2446.
- Kirschning, A.; Monenschein, H.; Wittenberg, R. The “Resin-Capture-Release” Hybrid Technique: A Merger between Solid- and Solution-Phase Synthesis. *Chem. Eur. J.* **2000**, *6*, 4445–4450.
- For a preliminary account of the establishment of this strategy see: Rosenbaum, C.; Müller, O.; Baumhof, P.; Mazitschek, R.; Giannis, A.; Waldmann, H. Synthesis and Biological Evaluation of an Indomethacin-Library Reveals a New Class of Angiogenesis-Related Kinase Inhibitors. *Angew. Chem.* **2004**, *116*, 226–230; *Angew. Chem., Int. Ed.*, **2004**, *43*, 224–228.
- Greene, L. M.; Reade, J. L.; Ware, C. F. Rapid Colorimetric Assay for Cell Viability: Application to the Quantitation of Cytotoxic and Growth Inhibitory Lymphokines. *J. Immunol. Methods* **1984**, *70*, 257–268.

JM0499099